



Combining ligand-based and structure-based drug design approaches to study the structure-activity relationships of a β -carboline derivative series

T. Akabli¹ · H. Toufik¹ · A. Yasri² · H. Bih¹ · F. Lamchouri¹

Received: 3 April 2018 / Accepted: 31 May 2018 / Published online: 19 June 2018
© Springer Science+Business Media, LLC, part of Springer Nature 2018

Abstract

In this study, we investigated the structure-activity relationships of a series of β -carboline alkaloid derivatives using the 2D-QSAR and molecular docking, in order to identify the mode of interaction between β -carboline derivatives and the PLK1 kinase, and determine their key substituents responsible for the cytotoxic activity. The obtained QSAR models using multiple linear regression (MLR) and partial least squares (PLS) methods showed a high correlation between the experimental activity and the predicted one by PLS ($R^2_{\text{PLS}} = 0.82$, $q^2 = 0.72$) and MLR ($R^2_{\text{MLR}} = 0.82$, $q^2 = 0.72$). An external dataset was used to test the extrapolation power of the models which resulted in an $R^2_{\text{PLS}}(\text{EV}) = 0.76$; RMSE = 0.39. The 2D-QSAR analysis reveals that lipophilicity plays an important role in the cytotoxic activity of this group of β -carboline derivatives. Indeed, the molecular docking study into the active site of the polo-like kinase (PLK1) revealed that the most active ligand 57 shows higher binding energy and interacts, especially by H-bonds and hydrophobic interactions, with the active site of the PLK1 kinase. Consequently, the results obtained from the 2D-QSAR and docking studies provided a useful tool to design new and potent β -carboline derivatives as cytotoxic agents.

Keywords Alkaloids · β -Carbolines · 2D-QSAR · PLS · MLR · Molecular docking

Introduction

Alkaloids constitute the largest group of plant secondary metabolites containing nitrogen and exhibit extensive pharmacological actions, such as cytotoxic and antitumor activities [1, 2]. Furthermore, β -carbolines are a group of natural alkaloids that possess a common tricyclic skeleton [3, 4]. These compounds are produced and stored by plants as products of dif-

ferent biosynthesis pathways from amino acids such as lysine, ornithine, tyrosine, and tryptophan [5]. They are also encountered in some animals such as insects and mammals as well as human tissues and body fluids [6]. In recent decades, these compounds have attracted a great interest due to their pharmacological properties such as anxiolytic, hypnotic, anticonvulsant, sedative, antimicrobial, antiviral, parasitical, antidiabetic, and anti-inflammatory, as well as their potent antitumor activities [7–14]. Indeed, *in vitro* studies have demonstrated the decrease in cell viability of cancer cells from various tissues [15–23]. This anticancer activity is also confirmed *in vivo* since β -carbolines inhibit the tumor growth of various murine models [13, 15, 23–25]. In addition, the study by Zhiyong Chen and al., which examined the synthesis of a series of β -carboline derivatives, the evaluation of their antitumor activities, and the analysis of structure-activity relationships, showed that these compounds have potent antitumor activities, and that the antitumor potential is correlated to both the planarity of the molecule and the presence of the substituents on the central ring [26].

✉ T. Akabli
taoufik.akabli@usmba.ac.ma

✉ H. Toufik
hamid.toufik@usmba.ac.ma

¹ Laboratory of Materials, Natural Substances, Environment and Modeling (LMSNEM), Polydisciplinary Faculty of Taza, Sidi Mohamed Ben Abdellah University of Fez, Fez, Morocco

² AgroBioSciences Division, Mohammed VI Polytechnic University (UM6P), Benguerir, Morocco

This activity is explained by the action of β -carbolines on different characteristics acquired by cancer cells, through multiple mechanisms of action, namely:

- Inhibition of cyclin-dependent kinases (CDK), inducing a cell cycle arrest of different cancer cell lines. Thus, a state of senescence in breast cancer cells (MCF-7) by inhibiting the expression of telomerase [21].
- Increased expression of tumor suppressor factor (p53), inducing apoptosis, cell cycle arrest, and inhibition of angiogenesis [18, 21, 24].
- Inhibition of the regulated phosphorylated tyrosine kinase double-specified protein (DYRK1A) by degradation of the amplified and/or mutated epidermal growth factor receptor (EGFR) in glioblastomas, which will inhibit the growth of Tumor cells [27–29].
- Induction of cell death by decreasing expression of several anti-apoptotic proteins (Bcl-x1, Bcl-2, and Mcl-1) and increasing expression of pro-apoptotic proteins (Bid, Bax) [13, 18, 20, 22, 23]. Thus, it has been shown that β -carbolines inhibit topoisomerase 1, which causes transcriptional changes, inhibition of replication, and DNA damage-inducing cell death [29, 30].
- Inhibition of invasion, angiogenesis, and formation of metastases by the action of β -carbolines on the expression of various pro- and anti-metastatic and angiogenic factors [14, 22, 24].

Furthermore, it has been found that this class of molecule exhibits remarkable acute neurotoxicity in mice characterized by tremors, agitation, and convulsion movements [13, 31, 32].

As for targeted receptor of this chemical series, it has been shown that β -carbolines are potent inhibitors of polo-like kinases (PLK) which plays an essential role in the ordered execution of mitotic events [33]. PLK1 kinase, a member of the PLK family, is an attractive target for anticancer drugs.

In continuing of our work to develop novel more effective cytotoxic, antitumor, and less toxic agents from the β -carboline derivatives using experimental and theoretical studies [34–37], we studied a series of β -carboline derivatives exhibiting cytotoxic activity against the hepatocellular line (HepG2) using 2D-QSAR and molecular docking analysis. The aim of this study was to identify the mode of interaction between β -carboline derivatives and the PLK1 kinase and determine their key substituents responsible for the cytotoxic activity, in order to guide the design of new β -carboline alkaloids with improved pharmacological activities and less neurotoxicity.

Materials and methods

Data collection

In this study, all β -carboline derivatives (40 molecules) have been taken from the work of Cao et al. [32]. The reported IC_{50} values for cytotoxic activity against the hepatocellular line (HepG2) were converted into the corresponding pIC_{50} values ($pIC_{50} = -\log IC_{50}$) and selected for this study (Table 1). Dataset was split into two sets; 34 molecules were chosen randomly to develop the QSAR model (training set) and the rest (7 molecules) were used to test the prediction performance of the proposed model (test set).

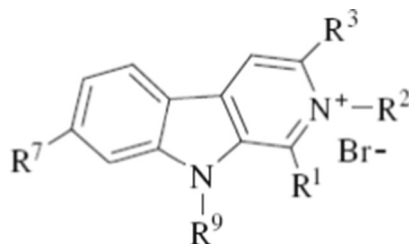
Molecular modeling

2D QSAR modeling

All compounds were sketched using the MarvinSketch program (version 16.2.1.0) [38], and various 2D descriptors were calculated using the MOE software (Molecular Operating Environment version 2008.10) [39]. After the calculation of descriptors provided by MOE software, a correlation matrix for variable selection was applied on the molecular descriptors to select only the appropriate ones. Therefore, the number was reduced to six descriptors which are used as input to perform multiple linear regression (MLR) and partial least squares (PLS) methods using MOE and XLSTAT 2014 software package [40], respectively. Subsequently, the quality of the models developed was examined by different statistical parameters [41], for instance, the square of correlation coefficient (R^2), adjusted coefficient of determination (R^2_{adj}), root mean square error (RMSE), and variance ratio (F) at specified degrees of freedom (df). In addition, the models were validated using internal cross-validation (q^2) and external validation (R^2_{pred}). [42–44]

Docking study

To explore the interaction and illustrate the accurate binding model for the active site of the PLK1 with ligands, a molecular docking study was performed using AutodockVina and Autodock tools 1.5.4 [45]. The X-ray crystal structure of the PLK1 (PDB code 2OWB) was used for the docking study. All small molecules were removed from the protein, and the receptor was used for the docking study by adding the polar hydrogen to assign appropriate ionization states to both acidic and basic amino acid residues. For ligands, they were sketched using the MarvinSketch program and minimized by MOE software, using MMFF94 (Merck Molecular Force Field) force field with the gradient convergence criterion set to 0.01 kcal/mol, and saved in pdb format. Then, four compounds (57, 58, 59, and 60) with better activity were docked

Table 1 Chemical structures and activities (pIC₅₀ on HepG2 cell line) of the studied β -carboline derivatives

Name	pIC ₅₀ (HepG2)	R ₁	R ₂	R ₃	R ₇	R ₉
compound1	3,777	3,4,5-trimethoxyphenyl	-	CO ₂ C ₂ H ₅	H	H
Compound2	3,682	3,4,5-trimethoxyphenyl	-	CO ₂ H	H	<i>n</i> -C ₄ H ₉
Compound3*	4,058	3,4,5-trimethoxyphenyl	-	CONH(CH ₂) ₂ OH	H	<i>n</i> -C ₄ H ₉
Compound4	4,081	H	-	CONH(CH ₂) ₂ NH ₂	H	<i>n</i> -C ₄ H ₉
Compound5	4,019	H	-	CONH(CH ₂) ₆ NH ₂	H	<i>n</i> -C ₄ H ₉
Compound6	3,854	CH ₃	-	CONH(CH ₂) ₂ OH	H	<i>n</i> -C ₄ H ₉
Compound7*	4,66	CH ₃	-	CONH(CH ₂) ₂ NH ₂	H	<i>n</i> -C ₄ H ₉
Compound8	4,458	CH ₃	-	CONH(CH ₂) ₂ NH ₂	H	CH ₂ C ₆ H ₅
Compound9	3,983	H	-	CONH(CH ₂) ₂ NH ₂	H	CH ₂ C ₆ H ₅
Compound10	4,231	H	-	CONH(CH ₂) ₆ NH ₂	H	CH ₂ C ₆ H ₅
Compound11	3,893	H	-	CH ₂ OH	H	<i>n</i> -C ₄ H ₉
Compound12*	3,845	CH ₃	-	CHO	H	<i>n</i> -C ₄ H ₉
Compound13	4,158	CH ₃	CH ₂ C ₆ H ₅	H	H	H
Compound14	4,481	CH ₃	(CH ₂) ₃ C ₆ H ₅	H	H	H
Compound15*	4,276	CH ₃	CH ₂ C ₆ H ₅	CO ₂ C ₂ H ₅	H	H
Compound16	4,263	CH ₃	CH ₂ C ₆ H ₅	H	OCH ₃	H
Compound17	4,027	H	<i>n</i> -C ₄ H ₉	H	H	H
Compound18	4,112	H	CH ₂ C ₆ H ₅	H	H	H
Compound19	4,351	H	(CH ₂) ₃ C ₆ H ₅	H	H	H
Compound20	3,873	CH ₃	-	H	OH	C ₂ H ₅
Compound21	4,089	CH ₃	-	H	OH	<i>n</i> -C ₄ H ₉
Compound22	3,936	CH ₃	-	H	OH	<i>i</i> -C ₄ H ₉
Compound23	4,548	CH ₃	-	H	OH	(CH ₂) ₃ C ₆ H ₅
Compound24*	4,162	CH ₃	-	H	OC ₂ H ₅	C ₂ H ₅
Compound25	3,627	CH ₃	-	H	OCH ₂ C ₆ F ₅	C ₂ H ₅
Compound26	4,364	CH ₃	-	H	OC ₂ H ₅	<i>n</i> -C ₄ H ₉
Compound27	4,52	CH ₃	-	H	OCH(CH ₃) ₂	<i>n</i> -C ₄ H ₉

Table 1 (continued)

Compound28	4,81	CH ₃	-	H	OC ₄ H ₉	<i>n</i> -C ₄ H ₉
Compound29	3,896	CH ₃	-	H	OC ₁₀ H ₂₁	<i>n</i> -C ₄ H ₉
Compound30	4,917	CH ₃	-	H	OC ₄ H ₉	<i>i</i> -C ₄ H ₉
Compound31	4,654	CH ₃	-	H	OCH ₂ C ₆ H ₅	<i>i</i> -C ₄ H ₉
Compound32	4,836	CH ₃	-	H	OCH(CH ₃) ₂	(CH ₂) ₃ C ₆ H ₅
Compound33	3,979	CH ₃	-	H	OC ₈ H ₁₇	(CH ₂) ₃ C ₆ H ₅
Compound34	4,804	CH ₃	-	H	OCH ₂ C ₆ H ₅	(CH ₂) ₃ C ₆ H ₅
Compound35	3,833	CH ₃	-	H	OCH ₂ C ₆ F ₅	(CH ₂) ₃ C ₆ H ₅
Compound36	4,845	CH ₃	CH ₂ C ₆ H ₅	H	OC ₂ H ₅	C ₂ H ₅
Compound37	5,796	CH ₃	CH ₂ C ₆ H ₅	H	OCH ₂ C ₆ F ₅	C ₂ H ₅
Compound38*	5,745	CH ₃	CH ₂ C ₆ H ₅	H	OC ₄ H ₉	<i>i</i> -C ₄ H ₉
Compound39	5,721	CH ₃	CH ₂ C ₆ H ₅	H	OCH ₂ C ₆ H ₅	<i>i</i> -C ₄ H ₉
Compound40	5,409	CH ₃	CH ₂ C ₆ H ₅	H	OC ₈ H ₁₇	(CH ₂) ₃ C ₆ H ₅

*Compounds contained within the test set

within the prepared protein. The mode of interaction of the co-crystallized ligand against 2OWB was used a standard docked model.

AutoGrid was carried out for the preparation of the grid map using a grid box to enclose the binding site with dimensions of $x=20$, $y=20$, and $z=20$ at 1 Å spacing. The Lamarckian genetic algorithm was used for the calculation of the docking possibilities. Then, the results were analyzed using Discovery studio 2016 and PyMol software's [46, 47].

Results and discussion

2D QSAR modeling

In this work, we used principal component analysis by XLSTAT 2014 software to select six descriptors that show a high correlation with the response activity and no correlation between them owing to the fact that the greatest value of the correlation coefficient is 0.75; this one gives extra weight because they will be more effective at prediction [48]. Figure 1 presents the circles of correlations corresponding to a projection of the six variables on a two-dimensional plane constituted by the two factors (F1 and F2). Besides, the principal component analysis also gives a representation of the molecules of the database in a plan composed by the first two principal components (F1 and F2), which can show the presence of three subgroups of molecules. As shown in Fig. 2, molecules without hydrogen bond donor or acceptor are identified at the bottom left of the graph. At the top of the graph

center, we can distinguish the group of molecules with one or two hydrogen bond acceptors and no hydrogen bond donor. Finally, molecules that have more than two hydrogen bond acceptors and one hydrogen bond donor are found at the bottom right of the graph.

From this first analysis, we can conclude that the number of hydrogen bond donor and acceptor is the main features for discriminating between the molecules within the overall database.

Thereafter, the QSAR model was performed using PLS and RLM methods correlating the cytotoxic activity with six

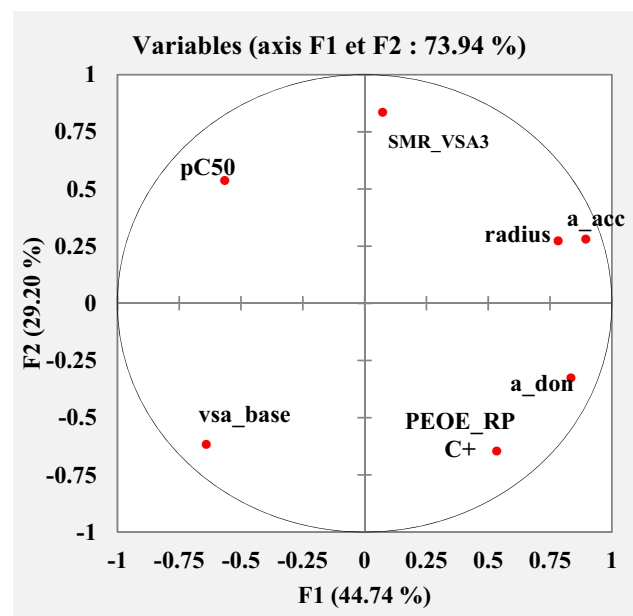


Fig. 1 Correlation circle of the descriptors and cytotoxic activity

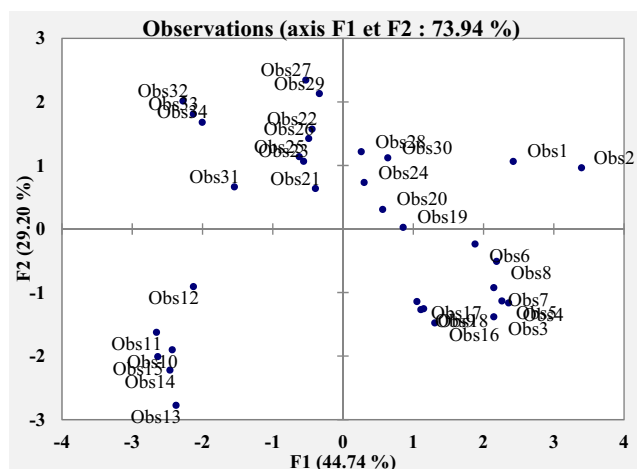


Fig. 2 Representation of the 34 molecules in the plan of the first two axes F1 and F2

descriptors. The generated models were thoroughly scrutinized for statistical validity and predictive potential, according to the criteria described in the experimental section.

The best QSAR model derived from modeling the cytotoxic activity of the 34 heterocyclic β -carboline derivatives is as follows.

RLM model:

$$pIC_{50} = 6.158 - 0.121 \times radius - 10.536 \times PEOE_RPC^+ - 0.337 \times a_acc + 0.033 \times SMR_VSA3 - 0.179 \times vsa_base + 0.548 \times a_don$$

$N = 34 \quad R^2 = 0.82 \quad R^2_{adj} = 0.78 \quad RMSE = 0.254 \quad F = 20.848$

PLS model:

$$pIC_{50} = 6.158 - 0.121 \times radius - 10.536 \times PEOE_RPC^+ - 0.337 \times a_acc + 0.033 \times SMR_VSA3 - 0.179 \times vsa_base + 0.548 \times a_don$$

$N = 34 \quad R^2 = 0.82 \quad R^2_{adj} = 0.78 \quad RMSE = 0.227 \quad F = 20.85$

where N is the number of training set, R^2 is the squared correlation coefficient, R^2_{adj} is the adjusted coefficient of determination, RMSE is the root mean square error, and F represents the Fisher ratio between the variances of calculated and observed activities.

QSAR models were established using two statistical analysis methods (RLM and PLS), using experimental data (pIC_{50}) for a series of β -carboline derivatives and a set of six descriptors. The model selection criteria were based on the correlation coefficient values derived from the correlation between the experimental and predicted activities, as well as the inter-correlations between the descriptors.

We found that for both methods used (PLS, RLM), the QSAR model obtained can predict about 82% of the experimental activity (pIC_{50}) of the molecules. In addition, it has a high Fischer factor ($F = 20.848$) and a low error ($RMSE_{RLM} = 0.254$, $RMSE_{PLS} = 0.227$), which means that the model

explains the activity (dependent variable) in a statistically significant and satisfactory manner. The value of the test (t) is used to evaluate the importance of the descriptors involved in the model, which is in the following order:

$$PEOE_RPC^+ > vsa_base > radius > a_don > a_acc > SMR_VSA3.$$

A comparison of the quality of two models from MLR and PLS models (Table 2) shows that the PLS model outperforms slightly the MLR one when judged by the obtained RMSE values [49]. As PLS is a more robust multivariate statistical technique, we choose to use the PLS model as an *in silico* tool to predict the activity of β -carboline derivatives and to draw a SAR map for further design and chemical synthesis studies.

Taking into consideration the selected descriptors and their impacts on the PLS model, we were able to propose a structure-activity relationship map that highlights the structural motifs responsible for the cytotoxic activity of the β -carboline derivatives (Fig. 3):

Structure-activity relationship (SAR) analysis shows that the activity of the β -carboline derivatives can be influenced by:

- The planarity of the molecule that was captured in part by the *radius* descriptor in agreement with the published work by Zhiyong Chen and al [26];
- The electropositive character, captured by the descriptor *vsa_base*, of the nitrogen atom in position 2; and
- The presence of various substituents on the structure of the β -carbolines essentially represented by the *SMR_VSA3* descriptor.

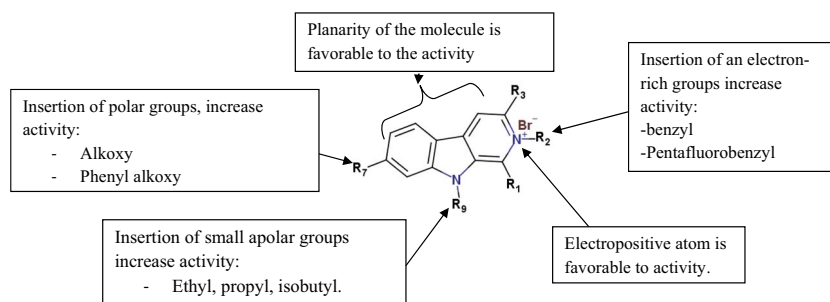
The QSAR model revealed that the activity of β -carboline derivatives was represented by some of selected descriptors:

- The number of hydrogen bond acceptor (*a_acc*) has a negative coefficient in the model equation, suggesting that increased activity can be achieved by decreasing the number of heteroatoms (nitrogen or oxygen atoms);
- The number of hydrogen bond donor (*a_don*) has a positive coefficient in the model equation, suggesting that an

Table 2 Values of determination coefficients and mean square errors obtained by the RLM and PLS models

	PLS		RLM	
	R^2	RMSE	R^2	RMSE
Training set	0.82	0.227	0.82	0.254
Test set	0.76	0.390	0.76	0.393

Fig. 3 Structure-activity relationship of the β -carboline derivatives



increase in activity can be achieved by increasing heteroatoms with one or more hydrogen atoms;

- The relative partial positive charge (PEOE_RPC+) obtained using the partial equalization of orbital electronegativities (PEOE) method is defined as the ratio of the largest positive partial charge to the total positive partial charge on the molecule [50]. This descriptor has a negative coefficient in the model equation, suggesting that increased activity can be obtained by decreasing the relative partial positive charge.
- The basic character (vsa_base) of the molecules has a negative coefficient in the model equation, suggesting that increased activity can be obtained by increasing the polarity of the β -carboline derivatives;
- Radius (radius) has a negative contribution to activity, which means that activity is improved by decreasing the radius. Thus, molecules that have an ionic bond between nitrogen and bromine (no path between the two atoms) have the smallest radius (radius = 0), suggesting that the positive charge of pyridinium is favorable to cytotoxic activity;
- Molar refractivity based on approximate Van Der Waals surface area calculations (SMR_VSA3) is usually used to reflect the polarizability of molecule [51]. The positive sign of this descriptor suggests that the polarizability of the molecule is favorable for the cytotoxic activity.

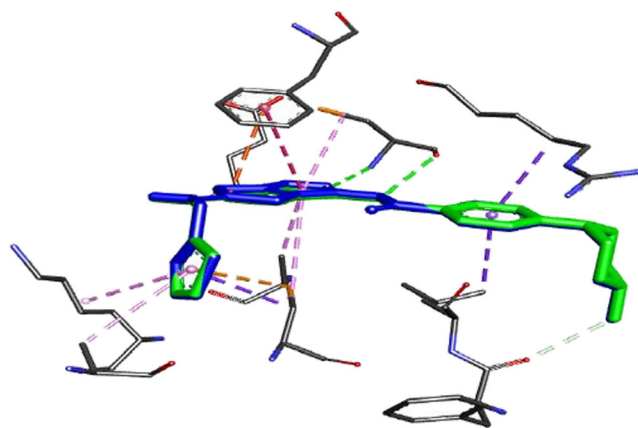


Fig. 4 Redocking pose and docking interactions of co-crystallized compound (green = original, blue = docked)

Molecular docking

Docking study was carried out on the four most active compounds (57, 58, 59, 60) to identify the nature of the interactions between ligand and biological target taking into account the orientation and conformation of the ligand in the active site of the protein. In this study, docking protocol was validated by redocking of the co-crystallized ligand at the PLK1 kinase (Fig. 4). The RMSD (root mean square distance) of the docked ligand was within the reliable range of 2 Å, suggesting that the docking procedure could be used to predict the binding mode of our compounds.

The interaction analysis of the ligand-protein indicates that important residues present at the binding site were polar (Lys66, Asp194, Arg57, Arg134, Lys61, Lys82, Arg136, Cys67, Glu131, Cys133) and non-polar (Leu132, Val114, Leu130, Gly62, Ala65, Leu59, Phe58, Phe183, Ala80). As shown in Fig. 4, we can see that the co-crystallized compound sits in the hydrophobic cavity and interacts by several types of interactions and more precisely by the conventional hydrogen bond with Glu131 and Cys133.

The ligands studied show a strong binding to the active sites of the target. As reported in Table 3, the biological activity values correlate with the estimated binding energy and the latter decrease with the increase of biological activity.

The analysis of interactions between the compound 57 and the binding site (Fig. 5) reveals that is surrounded by the hydrophobic region formed by Arg135, Arg134, Arg57, Glu69, Cys133, Gly193, and His105. Also, compound 57 exhibits a hydrogen binding interactions between three fluorines and oxygen of the pentafluorobenzyl moiety with Cys67 and Asp194 of PLK1. In another hand, compound 57 interacts with PLK1 by other binds such as Pi-sigma, Alkyl, Pi-Alkyl,

Table 3 Activity of the studied compounds and their binding energy

Compounds	pIC ₅₀	Binding energy
Compound 57	5796	– 8.4
Compound 58	5745	– 8.2
Compound 59	5721	– 8.2
Compound 60	5409	– 7.7

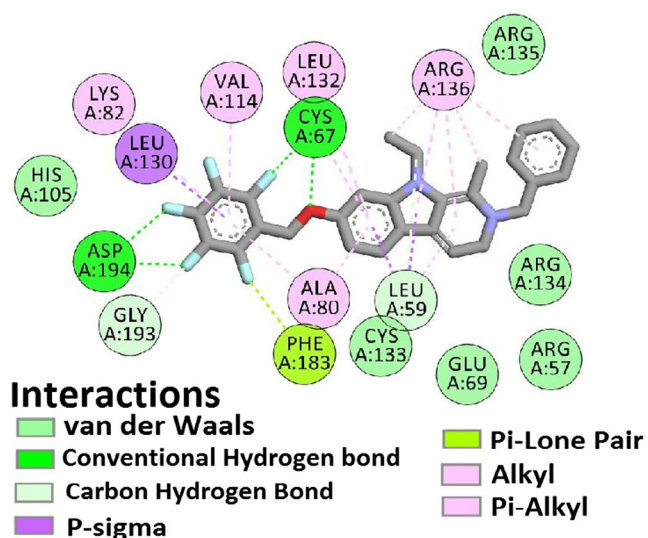


Fig. 5 Interactions between the most active compound (57) with PLK1 receptor, visualized with Discovery studio visualizer program

and Pi-lone Pair with Leu130, Lys82, Val114, Leu132, Arg136 Ala80, and Phe183.

The results obtained during this work correlate well with each other and are in good agreement with those of the 3D-QSAR obtained by Cao et al. [32]. In fact, the electropositive parameter captured by 3D-QSAR in position 2 can be represented by the descriptor *vsa_base* obtained by the 2D-QSAR model; then, the presence of the electron-rich groups in positions 2 and 7 such as benzyl and pentafluorobenzyl, respectively, is favorable for cytotoxic activity since they make it possible to form pi-alkyl and alkyl bonds with PLK1. In addition, docking results show that the pentafluorobenzyl moiety plays a crucial role in improving binding energy by forming hydrogen bonds with PLK1, which can be captured by the selection of hydrogen bond donor and polarizability (*a_don*, *SMR_VSA3*) descriptors in 2D-QSAR which have a positive sign in the model. On the other hand, electrostatic repulsive interaction in position 3 due to the electronegative groups demonstrated by 3D-QSAR is unfavorable for cytotoxic activity; this may be explained by the negative sign obtained by 2D-QSAR for *PEOE_RPC⁺* descriptor.

According to the above findings, three compounds were designed based on the structure of the compounds with the

Table 4 Newly designed compound structures and their predictive activity and binding energy

Compound d	Structure	Predicted pIC50	Binding energy (kcal/mol)
1		5.88	-8.9
2		5.92	-9.7
3		6.06	-10.6

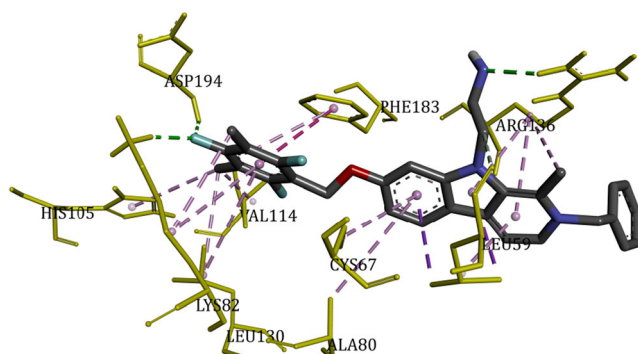


Fig. 6 Interactions between compound 3 with PLK receptor, visualized with Discovery studio visualizer program

highest pIC_{50} values (57). The structures of the compounds designed, the pIC_{50} values theoretically predicted by the 2D QSAR, and their binding energy are listed in Table 4. According to the results of the predicted activities, it was observed that the compounds designed had higher predicted pIC_{50} values than the compounds studied in this work. Furthermore, newly designed compounds were docked at the PLK1 kinase. All compounds have better binding energy than the compounds studied in this work since they were well placed in the active site and indicate that they could be potential inhibitors of PLK1 kinase. The interaction analysis between the compound 3, which showed the highest activity and the low binding energy, and the PLK1 kinase reveals that the introduction of the methyl group in the meta-benzyl positions at the position 7 and the substitution of the ethyl group in position 9 with the amino group allow forming hydrophobic binding and establishing three hydrogen bonds (two bonds between fluorine and Lys82 and Asp194 and one bond between the amino group and Arg136) as well as other bonds: alkyl, Pi-Alkyl, Pi-sigma, and Pi-Pi Stacked with Val114, Cys67, Ala80, Leu130, His105, Leu59, and Phe183, respectively, as shown in Fig. 6.

Conclusions

In this paper, a quantitative analysis of structure-activity relationships and molecular docking studies was performed on a series of 40 β -carboline derivatives. The 2D-QSAR was performed using partial least squares regression (PLS) and multiple linear regression (RLM). The results found showed that the model proposed via the PLS method is able to accurately predict the cytotoxic activity and that the selected descriptors are relevant to explain the increase or decrease in cytotoxic activity against the hepatocellular (HepG2) line. In addition, the docking study showed that compound 57 has low binding energy and seems to have more binding affinities towards PLK1. Analysis of the structural interactions shows that this compound is in a hydrophobic pocket and interacts with the

active site, especially through hydrogen bonds. Accordingly, obtained results were used to design three newly compounds with predicted low binding affinity and improved cytotoxic activity. Overall, these results can be used to perform virtual screening for new β -carboline and can also help to design new compounds to obtain potent and novel β -carboline with improved biological activities.

Compliance with ethical standards

Conflict of interests The authors declare that they have no conflict of interest.

Ethical approval This chapter does not contain any studies with human participants or animals performed by any of the authors.

References

- Mohan K, Jeyachandran R, Deepa (2012) Alkaloids as anticancer agents. *Ann Phytomed* 1:46–53
- Byler KG, Wang C, Setzer WN (2009) Quinoline alkaloids as intercalative topoisomerase inhibitors. *J Mol Model* 15:1417–1426. <https://doi.org/10.1007/s00894-009-0501-6>
- Abramovitch RA, Spenser ID (2008) The carbolines. *Adv Heterocycl Chem* 3:79–207. [https://doi.org/10.1016/S0065-2725\(08\)60542-5](https://doi.org/10.1016/S0065-2725(08)60542-5)
- Gilbert J, Senyuva HZ (2008) *Bioactive compounds in foods*. Blackwell Pub, Oxford
- Aniszewski T (2015) *Alkaloids: chemistry, biology, ecology, and applications* 2nd edn. Elsevier, Waltham, MA
- Zheng W, Wang S, Barnes LF et al (2000) Determination of harmine and harmine in human blood using reversed-phased high-performance liquid chromatography and fluorescence detection. *Anal Biochem* 279:125–129. <https://doi.org/10.1006/abio.1999.4456>
- Braestrup C, Nielsen M, Olsen CE (1980) Urinary and brain beta-carboline-3-carboxylates as potent inhibitors of brain benzodiazepine receptors. *Proc Natl Acad Sci* 77:2288–2292
- Schupp P, Poehner T, Edrada R et al (2003) Eudistomins W and X, two new β -carbolines from the micronesia tunicate *Eudistoma* sp. *J Nat Prod* 66:272–275. <https://doi.org/10.1021/np020315n>
- Nazari Formaggio AS, Santos PR, Zanolli K et al (2009) Synthesis and antiviral activity of β -carboline derivatives bearing a substituted carbonylhydrazide at C-3 against poliovirus and herpes simplex virus (HSV-1). *Eur J Med Chem* 44:4695–4701. <https://doi.org/10.1016/j.ejmech.2009.07.005>
- Di Giorgio C, Delmas F, Ollivier E et al (2004) In vitro activity of the β -carboline alkaloids harmine, harmine, and harmaline toward parasites of the species *Leishmania infantum*. *Exp Parasitol* 106:67–74. <https://doi.org/10.1016/j.exppara.2004.04.002>
- Waki H, Park KW, Mitro N et al (2007) The small molecule harmine is an antidiabetic cell-type-specific regulator of PPAR γ expression. *Cell Metab* 5:357–370. <https://doi.org/10.1016/j.cmet.2007.03.010>
- Yamazaki Y, Kawano Y (2011) Inhibitory effects of herbal alkaloids on the tumor necrosis factor- α and nitric oxide production in lipopolysaccharide-stimulated RAW264 macrophages. *Chem Pharm Bull (Tokyo)* 59:388–391
- Chen Q, Chao R, Chen H et al (2005) Antitumor and neurotoxic effects of novel harmine derivatives and structure-activity relationship analysis. *Int J Cancer* 114:675–682. <https://doi.org/10.1002/ijc.20703>

14. Cao R, Peng W, Chen H et al (2005) DNA binding properties of 9-substituted harmine derivatives. *BiochemBiophys Res Commun* 338:1557–1563. <https://doi.org/10.1016/j.bbrc.2005.10.121>
15. Cao R, Chen Q, Hou X et al (2004) Synthesis, acute toxicities, and antitumor effects of novel 9-substituted β -carboline derivatives. *Bioorg Med Chem* 12:4613–4623. <https://doi.org/10.1016/j.bmc.2004.06.038>
16. Pérez Martín JM, Labrador V, Fernández Freire P et al (2004) Ultrastructural changes induced in HeLa cells after phototoxic treatment with harmine. *J Appl Toxicol* 24:197–201. <https://doi.org/10.1002/jat.972>
17. Song Y, Kesuma D, Wang J et al (2004) Specific inhibition of cyclin-dependent kinases and cell proliferation by harmine. *BiochemBiophys Res Commun* 317:128–132. <https://doi.org/10.1016/j.bbrc.2004.03.019>
18. Hamsa TP, Kuttan G (2011) Harmine activates intrinsic and extrinsic pathways of apoptosis in B16F-10 melanoma. *Chin Med* 6:11
19. Frédéric R, Bruyère C, Vancaeynest C et al (2012) Novel trisubstituted harmine derivatives with original in vitro anticancer activity. *J Med Chem* 55:6489–6501. <https://doi.org/10.1021/jm300542e>
20. Liu H, Han D, Liu Y et al (2013) Harmine hydrochloride inhibits Akt phosphorylation and depletes the pool of cancer stem-like cells of glioblastoma. *J Neuro-Oncol* 112:39–48. <https://doi.org/10.1007/s11060-012-1034-x>
21. Zhao L, Wink M (2013) The β -carboline alkaloid harmine inhibits telomerase activity of MCF-7 cells by down-regulating hTERT mRNA expression accompanied by an accelerated senescent phenotype. *PeerJ* 1:e174. <https://doi.org/10.7717/peerj.174>
22. Zhang H, Sun K, Ding J et al (2014) Harmine induces apoptosis and inhibits tumor cell proliferation, migration and invasion through down-regulation of cyclooxygenase-2 expression in gastric cancer. *Phytomedicine* 21:348–355. <https://doi.org/10.1016/j.phymed.2013.09.007>
23. Cao M-R, Li Q, Liu Z-L et al (2011) Harmine induces apoptosis in HepG2 cells via mitochondrial signaling pathway. *Hepatobiliary Pancreat Dis Int* 10:599–604. [https://doi.org/10.1016/S1499-3872\(11\)60102-1](https://doi.org/10.1016/S1499-3872(11)60102-1)
24. Dai F, Chen Y, Song Y et al (2012) A natural small molecule harmine inhibits angiogenesis and suppresses tumour growth through activation of p53 in endothelial cells. *PLoS One* 7:e52162. <https://doi.org/10.1371/journal.pone.0052162>
25. Hamsa TP, Kuttan G (2011) Studies on anti-metastatic and anti-invasive effects of harmine using highly metastatic murine B16F-10 melanoma cells. *J Environ Pathol Toxicol Oncol* 30:123–137. <https://doi.org/10.1615/JEnvironPatholToxicolOncol.v30.i2.40>
26. Chen Z, Cao R, Shi B et al (2011) Synthesis and biological evaluation of 1,9-disubstituted β -carbolines as potent DNA intercalating and cytotoxic agents. *Eur J Med Chem* 46:5127–5137. <https://doi.org/10.1016/j.ejmech.2011.08.027>
27. Bain J, Plater L, Elliott M et al (2007) The selectivity of protein kinase inhibitors: a further update. *Biochem J* 408:297–315. <https://doi.org/10.1042/BJ20070797>
28. Göckler N, Jofre G, Papadopoulos C et al (2009) Harmine specifically inhibits protein kinase DYRK1A and interferes with neurite formation: harmine, a specific inhibitor of DYRK1A. *FEBS J* 276:6324–6337. <https://doi.org/10.1111/j.1742-4658.2009.07346.x>
29. Adayev T, Wegiel J, Hwang Y-W (2011) Harmine is an ATP-competitive inhibitor for dual-specificity tyrosine phosphorylation-regulated kinase 1A (Dyrk1A). *Arch BiochemBiophys* 507:212–218. <https://doi.org/10.1016/j.abb.2010.12.024>
30. Sobhani AM, Ebrahimi S-A, Mahmoudian M (2002) An in vitro evaluation of human DNA topoisomerase I inhibition by Peganumharmala L. seeds extract and its beta-carboline alkaloids. *J Pharm PharmSci* 5:19–23
31. Cao R, Chen H, Peng W et al (2005) Design, synthesis and in vitro and in vivo antitumor activities of novel β -carboline derivatives. *Eur J Med Chem* 40:991–1001. <https://doi.org/10.1016/j.ejmech.2005.04.008>
32. Cao R, Guan X, Shi B et al (2010) Design, synthesis and 3D-QSAR of β -carboline derivatives as potent antitumor agents. *Eur J Med Chem* 45:2503–2515. <https://doi.org/10.1016/j.ejmech.2010.02.036>
33. Han X, Zhang J, Guo L et al (2012) A series of beta-carboline derivatives inhibit the kinase activity of PLKs. *PLoS One* 7:e46546. <https://doi.org/10.1371/journal.pone.0046546>
34. Lamchouri F, Settaf A, Cherrah Y et al (2000) In vitro cell-toxicity of *Peganumharmala* alkaloids on cancerous cell-lines. *Fitoterapia* 71:50–54
35. Lamchouri F, Toufik H, Elmalki Z et al (2013) Quantitative structure–activity relationship of antitumor and neurotoxic β -carbolines alkaloids: nine harmine derivatives. *Res ChemIntermed* 39:2219–2236. <https://doi.org/10.1007/s11164-012-0752-1>
36. Lamchouri F, Zemzami M, Jossang A et al (2013) Cytotoxicity of alkaloids isolated from *Peganumharmala* seeds. *Pak J Pharm Sci* 26:699–706
37. Lamchouri F, Toufik H, Bouzzine SM et al (2010) Experimental and computational study of biological activities of alkaloids isolated from *Peganum harmala* seeds. *J Mater EnvSci* 1:343–352
38. ChemAxon, MarvinSketch 2.1.0 (2016). <http://www.chemaxon.com>. Accessed 01 Dec 2017
39. Molecular Operating Environment software, Chemical Computing Group Inc., Montreal, Quebec, Canada. <http://www.chemcomp.com/>
40. Addinsoft (2014) XLSTAT: data analysis and statistical solution for microsoft excel. Paris, France. <http://www.xlstat.com>. Accessed 25 Feb 2017
41. Tropsha A (2010) Best practices for QSAR model development, validation, and exploitation. *Mol Inform* 29:476–488. <https://doi.org/10.1002/minf.201000061>
42. Dehmer M, Varmuza K, Bonchev D (2012) Statistical modelling of molecular descriptors in QSAR/QSPR: DEHMER:MOL. DESCRIPTOR O-BK. Wiley-VCH Verlag GmbH & Co. KGaA, Weinheim
43. Roy K (2007) On some aspects of validation of predictive quantitative structure–activity relationship models. *Expert Opin Drug Discov* 2:1567–1577. <https://doi.org/10.1517/17460441.2.12.1567>
44. Gramatica P (2007) Principles of QSAR models validation: internal and external. *QSAR Comb Sci* 26:694–701. <https://doi.org/10.1002/qsar.200610151>
45. Trott O, Olson AJ (2010) AutoDockVina: improving the speed and accuracy of docking with a new scoring function, efficient optimization, and multithreading. *J ComputChem* 31:455–461. <https://doi.org/10.1002/jcc.21334>
46. (2016) Dassault Systèmes BIOVIA, Discovery Studio Modeling Environment, Release 2017, San Diego: Dassault Systèmes. <http://accelrys.com/products/collaborative-science/bioviadiscoverystudio/>. accessed 01 Feb 2018
47. DeLano WL (2008) The PyMOL Molecular Graphics System, Version 2.0 Schrödinger, LLC. <http://www.pymol.org>. Accessed 01 Feb 2018
48. Consonni V, Ballabio D, Todeschini R (2010) Evaluation of model predictive ability by external validation techniques. *J Chemom* 24:194–201. <https://doi.org/10.1002/cem.1290>
49. Aptula AO, Jeliaskova NG, Schultz TW, Cronin MTD (2005) The better predictive model: high q^2 for the training set or low root mean square error of prediction for the test set? *QSAR Comb Sci* 24:385–396. <https://doi.org/10.1002/qsar.200430909>
50. Gasteiger J, Marsili M (1980) Iterative partial equalization of orbital electronegativity—a rapid access to atomic charges. *Tetrahedron* 36:3219–3288. [https://doi.org/10.1016/0040-4020\(80\)80168-2](https://doi.org/10.1016/0040-4020(80)80168-2)
51. Labute P (2000) A widely applicable set of descriptors. *J Mol Graph Model* 18:464–477. [https://doi.org/10.1016/S1093-3263\(00\)00068-1](https://doi.org/10.1016/S1093-3263(00)00068-1)